Non-destructive neutron structural studies of ancient ceramic fragments of the cultural heritage of the Republic of Kazakhstan

B.A. Bakirov[1,2], A.Zh. Zhomartova[*,1,3,4], S.E. Kichanov[1], R.S. Zhumatayev[5], A.T. Toleubayev[5], K.M. Nazarov[1,3,4], D.P. Kozlenko[1], A.M. Nazarova[5]

[1]Joint Institute for Nuclear Research, Dubna, Russia

[2]Kazan Federal University, Kazan, Russia

[3]L.N. Gumilyov Eurasian National University, Nur-Sultan, Kazakhstan

[4]Institute of Nuclear Physics Ministry of Energy of the Republic of Kazakhstan, Almaty, Kazakhstan

[5]Al-Farabi Kazakh National University, Almaty, Kazakhstan

E-mail: zhomartova@jinr.ru

The structural features of ancient ceramic fragments dating from various historical ages of ancient cultural groups inhabiting the territory of modern Kazakhstan were studied using optical microscopy, neutron diffraction, neutron tomography, and Raman spectroscopy methods. Fragments of ancient pottery were selected from the collection of ancient remains from archaeological excavations near Zaysan district of East Kazakhstan region, Republic of Kazakhstan. The phase analysis of the studied ceramics fragments was performed. Phases of feldspar, quartz and mica as additional additives for the manufacture of ancient pottery were observed. Minor phases of graphite, anatase, and calcite were detected. Structural features and spatial distribution of components inside the volume of ceramic fragments were studied. In some pottery fragments, organic additives, possibly of vegetable origin, were found. According to the obtained structural data, the specific features of ceramic manufacturing, as well as the processes of temperature annealing of pottery pieces are discussed.

Keywords: ancient ceramics; cultural heritage; non-destructive analysis; neutron diffraction; neutron tomography; Raman spectroscopy

Introduction

A significant number of ceramics remains found during various archaeological works can serve as a source of really valuable data on everyday life, the evolution of manufacturing or technologies, trade or conquest relations of certain civilizations or ethnic history [1]. The quality of ceramic products, the type of design or decorative patterns, as well as the chemical and mineral composition of raw clay materials, can open up wide opportunities for reliable historical identification of cultural heritage items or reconstruction of technological and manufacturing techniques of a particular historical period or cultural areas [2, 3]. It should be noted that the rather complex composition of clay, a wide variety of reinforcing additives, and the puzzling evolution of ceramic manufacturing technologies make it difficult to identify a certain general formation model for a diversity of ceramic remains. Nowadays, archeological scientific communities need to perform routine detailed studies of numerous ceramic objects in order to accumulate the necessary data for a database of knowledge on pottery materials for the purpose of improving identification procedures and finding correlations. From this point of view, the possibilities of experimental neutron methods of nondestructive structural diagnostics are of increasing interest [4-6]. The fundamental features of neutron interactions with matter determine the high penetration power, sensitivity to hydrogen-containing materials, and a good radiographic contrast between neighboring elements [7-9]. Along with classical traditional approaches, these methods provide reliable data on the chemical and mineral composition of ceramic samples, the spatial distribution of internal chemical or structural components, and the phase composition of raw clay materials [10-12]. The non-destructive nature of these methods, when valuable objects of cultural heritage completely retain their original state, attracts more and more researchers.

For our non-destructive structural studies, we selected several ceramic fragments of an almost unexplored historical community of ancient Saka tribes living on the territory of eastern modern Kazakhstan [13]. The objects of material culture of this ancient community belong to the Andronovo culture [14]. It is assumed that the Kazakh ethnogenesis was formed within the framework of autochthonous "Saka-Turkic" hypotheses, according to which the Saka and Turkic tribes inhabited the steppes of Central Asia since ancient times. Burial mounds, ruins of buildings, ancient metal and ceramic artifacts were found on the territory of Tarbagatay and Zaysan regions of East Kazakhstan [15]. The first archeological works in this place were carried out in 1734 by prominent scientists G.F. Miller and in 1793 by the botanist I. Sivers [16]. A more complete and detailed work related to several settlements, burial grounds, and burial mounds in the region of East Kazakhstan was performed by Prof. Chernikov [16]. Currently, since 2003, the archaeological dig has been performed under the supervision of D.K. Akhmetov [17]. Several large, one medium, and twenty small burial mounds have been studied [18]. One of the latest finds is a rich collection of fragments of ceramic ware. A preliminary study has already shown that the obtained ceramic fragments of pottery items belong to different historical epochs and cultural

layers. In the present investigation, the internal structural features of ceramic fragments of ancient pottery of Kazakh ethnicity were comprehensively studied using neutron diffraction and tomography methods, supported by conventional optical microscopy and Raman spectroscopy.

Materials and methods

Sample description

To represent the historical evolution of ancient ethnicities of East Kazakhstan, we selected ten fragments of ceramics dating from various historical and cultural eras. There is the Bronze Age, which corresponded to the Andronov culture; the Early Iron Age relates to the nomads of Berelian age; the Middle Ages corresponded to the Turks and Mongols periods. Photos of studied ceramic fragments are shown in Figure 1. There are remains of ancient pots that were found in the burial places of the archaeological excavations of Zhaipak, Eleke Sazi, Ainabulak, and Sabirbai [19]. A brief description of the ceramic samples and their tentative assignment to a certain historical period are presented in Table 1.

Table 1.
Numbering of the samples, collection code with the archeological location, estimated historical period and a brief description of the studied ceramic samples.

№	Sample code	Period	Description
1 2	Zhaipak big Zhaipak small	the Middle Ages	Ceramic fragments from the medieval settlement of Zhaipak, located in the Alakol area of Almaty region, Kazakhstan
3 4	Eleke Sazi 5 Eleke Sazi 6	the Early Iron Age	Mound Eleke Sazi is located in the Tarbagatay district of the East Kazakhstan region, belongs to the early Iron Age.
5	Ainabulak 11	the Bronze Age	Ceramic finds from a Bronze Age burial mound. The monument is located in the Zaysan district of the East Kazakhstan region.
6 7 8 9 10	Sabirbai 2(1) Sabirbai 2(2) Sabirbai 2(3) Sabirbai 2(A) Sabirbai 2(C)	the Bronze Age	Ceramic finds from the Bronze Age monument. The monument is located in the Tarbagatay district of the East Kazakhstan region.

Experimental methods

The photo images of the ceramic fragments with a maximum magnification of x12 were obtained using a Leica M165 microscope with a video camera set-up.
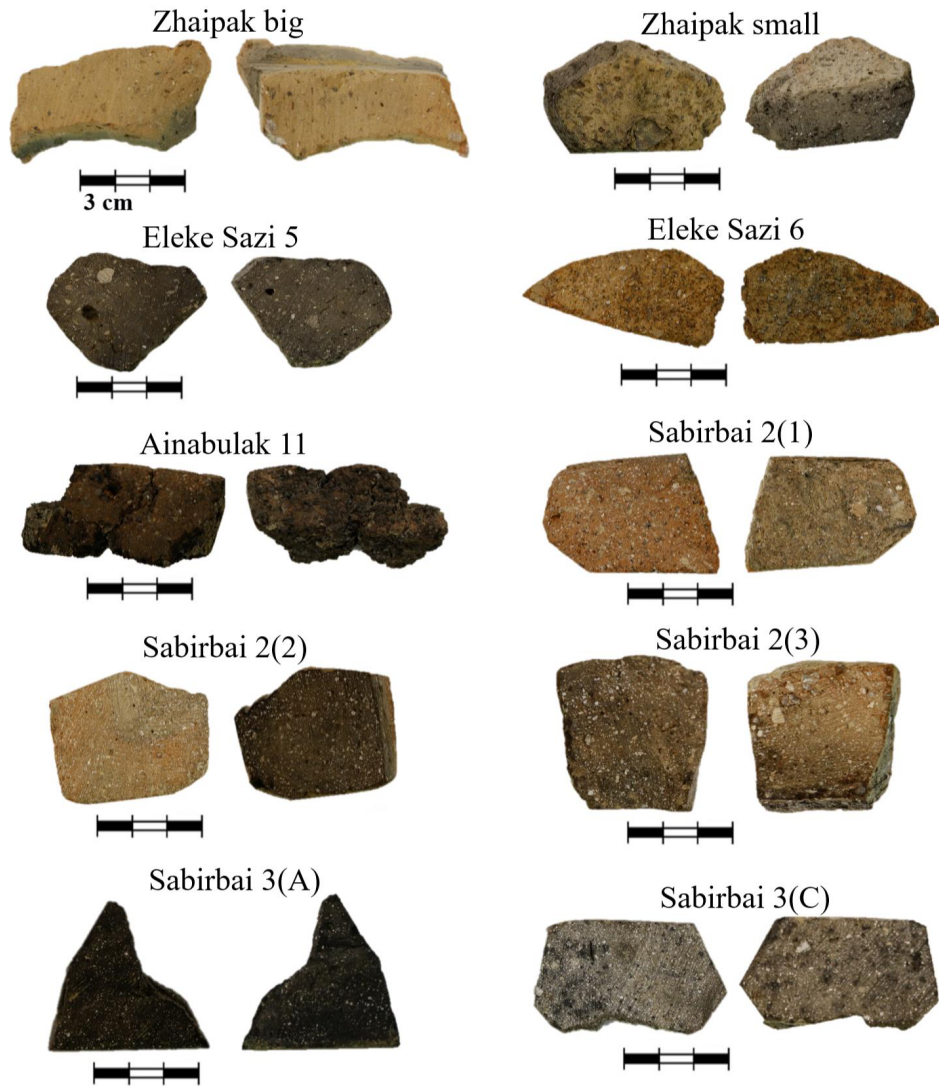
Figure 1. Photos of the studied ceramic samples. The scale bar of 3 cm is shown for each fragment.

The phase analysis of the ceramic fragments was performed using neutron diffraction experiments on the DN-6 neutron diffractometer of the IBR-2 pulsed reactor [20, 21]. The neutron powder diffraction data were taken at the scattering angle of $2\theta = 90°$. One neutron diffraction pattern was measured 20 min. The neutron diffraction data were analyzed using the FullProf software package [22].

Qualitative and quantitative raman spectra at room temperature were collected using a LabRAM HR spectrometer (Horiba Gr, France) with an excitation wavelength of 633 nm emitted by a He-Ne laser, 1800 grating, 200 μm confocal hole, and x20 lens. A set of Raman spectra was obtained from different local points on the surface of the fragments. Typical spectrum acquisition time was 10 min; measurement range was from 100 to 1600-1800 cm^{-1}. Tentative identification of the Raman spectra was performed by comparison with reference data from online databases [23].

Neutron tomographic experiments were carried out on a specialized NRT facility of the IBR-2 pulsed reactor [24]. A set of neutron radiography projections of ceramics was collected using a detector system based on a LiF/ZnS scintillation

screen and a high sensitivity Hamamatsu CCD camera (2048×2048 pixels). The camera was focused on a field of view of 100×100 mm^2; accordingly, the pixel size of the resulting image was 52×52 μm^2. For tomographic measurements, a Huber rotating table was used. The angle of rotation of the studied samples was $180°$ with a step of $0.5°$. The exposure time for one projection was 25 s, and the overall number of measured projections was 360. Using the ImageJ software package, the image data were nominated for the incident neutron beam, after being corrected by the camera's dark current [25]. For tomographic reconstructions, the STP (SYRMEP Tomo Project) program was used [26]. 3D volumetric data represent the spatial distribution of the neutron attenuation coefficients. The weakening of the neutron beam is formed due to the processes of neutron scattering and absorption during its interaction with the materials of the sample under study [27]. VGStudio MAX (Volume Graphics) software was used to visualize and analyze the reconstructed 3D models.

Results and discussion

Raman spectroscopy

To remove surface contamination and rough inhomogeneities from the side surface of the ceramic fragments, we slightly polished the side surface of the pottery remains. Enlarged images of side mechanical slices obtained using conventional optical microscopy are shown in Figure 2. The color of the fragments varies from a light-yellow sand color for the Zhaipak big sample to a dark one for the Sabirbai 3(A) fragment. Interestingly, on the slices of almost all samples, gray or black areas are clearly visible, which may relate to a violation of oxidative-reductive conditions due to an incomplete firing process [28]. Large coarse grains of inclusions with an average size range of 500-1400 μm are clearly visible on the slice of the ceramic samples. There is a black substance on the slice of the samples, most likely soot, which is formed during thermal annealing. The ceramic samples have a large number of pores and cracks about 1.0-5.0 mm in size.

The Raman spectroscopy was used for the identification of composite phases on the side slice of the studied pottery fragments. Several Raman spectra were collected from different points of the studied fragments. Figure 3 shows the Raman spectra of the observed phases of the ceramic fragments. The most intense Raman lines at 465, 354, 202, and 128 cm^{-1} are related to the α-quartz phase [29]. The Raman spectroscopy provides characteristics spectra, which correspond to the feldspar, calcate and anatase phases (Figure 3). Interestingly, quite a lot of carbon fractions were found (Figure 2) in the ceramic samples, which is associated with the presence of soot inside the ceramic samples. Carbon-containing soot can be formed by the combustion of organic elements during the annealing of pottery products. Recently, Bobrinsky proposed [30] a hypothesis about the existence of a technological method of adding some organic materials [31, 32]: animal manure, bird droppings, freshwater mollusks with their shells in the manufacture of ceramic products (Figure 4a). Based on the ratio of the intensity
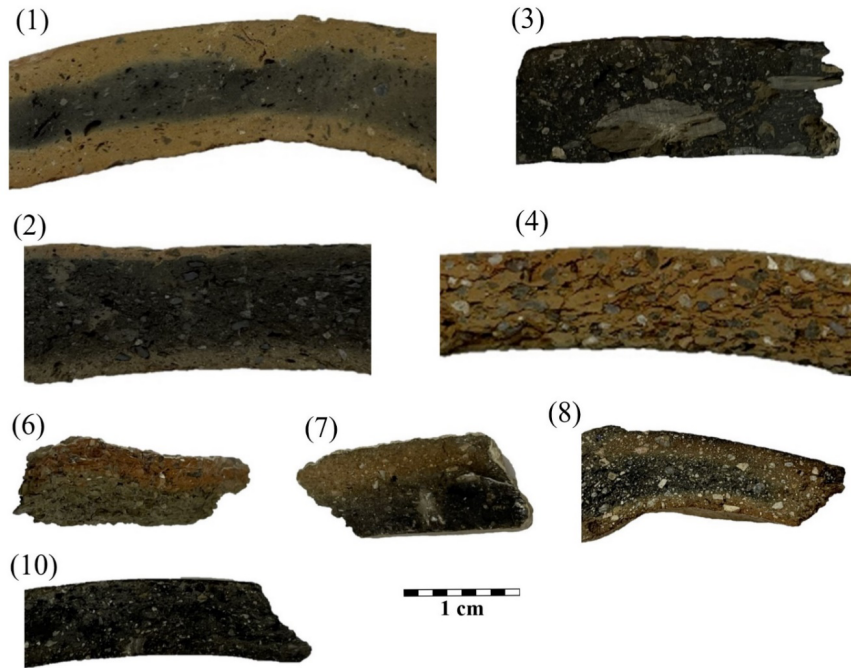
Figure 2. Microscope images of mechanical slices of the ceramic fragments.

of the Raman doublet of the carbon phase, the authors attempted to estimate the approximate dating of the ceramic samples [33]. The results of the calculated data are presented in Figure 4b.

The presence of different tracked composite phases in the studied ceramic fragments is shown in Table 2.

Table 2.
Phase composition according to Raman spectroscopy data for different ceramic fragments.

Sample	Phase composition				
	Quartz	Feldspar	Calcite	Carbon	Anatase
(1) Zhaipak big	+	+		+	+
(2) Zhaipak small	+	+		+	+
(3) Eleke Sazi 5	+			+	
(4) Eleke Sazi 6	+	+			+
(5) Ainabulak	+			+	+
(6) Sabirbai 1	+	+	+	+	
(7) Sabirbai 2	+	+	+	+	+
(8) Sabirbai 3	+	+			
(9) Sabirbai A	+	+		+	
(10) Sabirbai C	+	+		+	

Neutron diffraction

The phase composition inside the volume of the ceramic fragments was studied using the neutron diffraction method. As an example, Figure 5 shows two typical
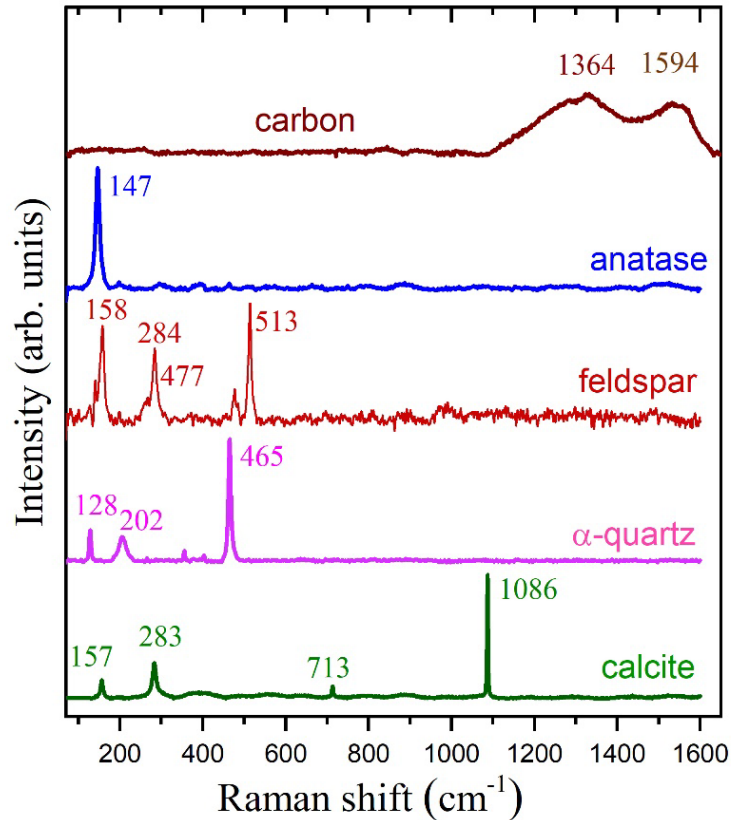
Figure 3. Characteristic Raman spectra obtained from different points of the mechanical slice of the studied ceramic fragments. The Raman wavenumbers of the most intense Raman peaks are indicated.
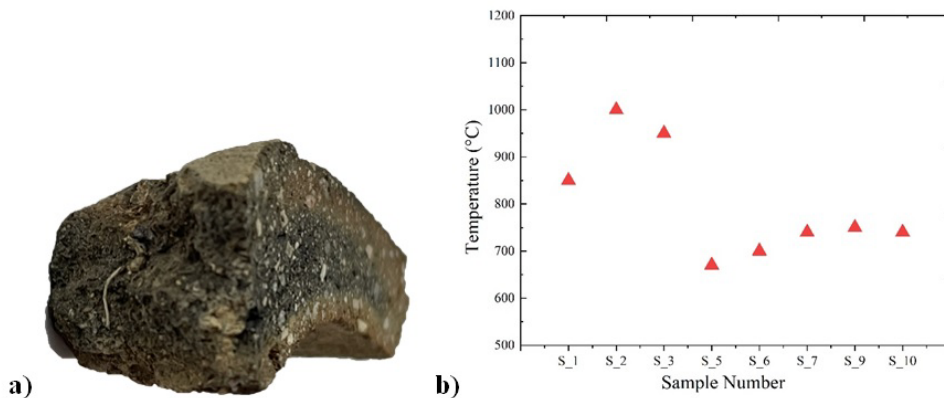

Figure 4. (a) Microscope image of Sample 8 with impurities of organic material. (b)Firing temperatures calculated from the ratio of Raman carbon peaks.

neutron patterns. The most intense diffraction peaks indicate a quartz phase [10, 34]. The crystal structure of this phase is described by the space group P3121 with unit cell parameters a = 4.908(5) Å and c = 5.414(4) Å, which corresponds to the previous data [35]. The second main phase in the composition of the ceramic fragments is mica with a trigonal crystal structure 1. The calculated unit cell parameters of mica phase are a = 8.163(9), b = 12.885(7), c = 7.241(9), $\alpha = 94.1(3)°$, $\beta = 116.8(2)°$, $\gamma = 87.8(1)°$ (for sample 1). The obvious presence of mica in the studied samples can be explained by the addition of granite chips in the form of crushed stone to clay masses during the manufacture of a ceramic product. It

should be noted that ancient settlements were located mainly in mountainous regions, where there was no access to sources of sea or river quartz sands [36]. This may indirectly indicate the local source of ceramic ware production and the rather closed nature of the tribes of East Kazakhstan.

There are some additional diffraction peaks on the neutron patterns (Figure 5). These peaks correspond to the feldspar phase. The crystal structure of this phase is described by the monoclinic C2/c symmetry with lattice parameters a = 5.187(6)Å, b = 9.307(5)Å, c = 20.181(1)Å, $\beta = 95.5(2)°$. Quartz and feldspar minerals are constituents of raw clay materials [34]. The volume content of the observed phases in the studied samples was calculated by the Rietveld method [22]. The obtained fractions of quartz, mica and feldspar phases are shown in Figure 6.
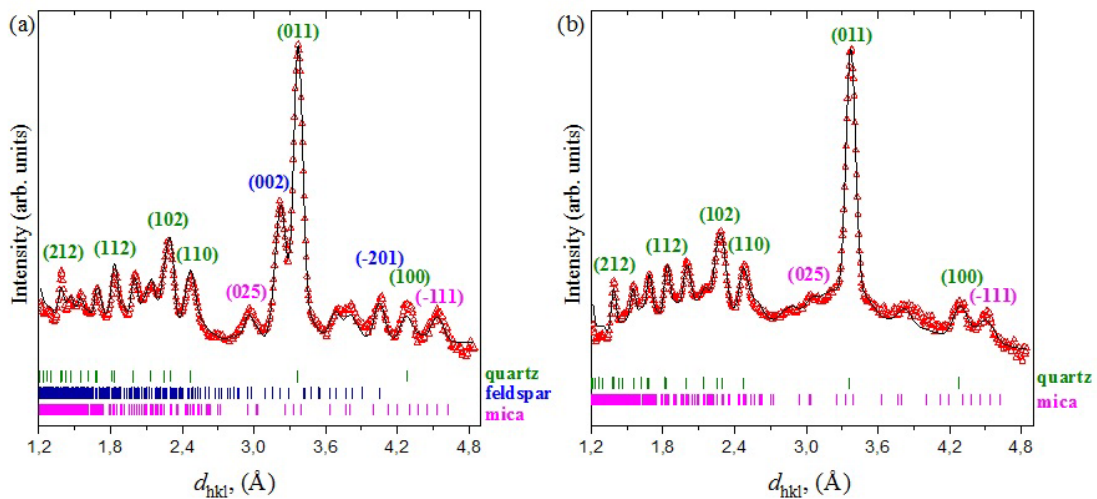

Figure 5. Two most representative neutron diffraction patterns of the ceramic fragments: Eleke Sazi 6 (a) and Eleke Sazi 5 (b). Experimental points and calculated profile are demonstrated. Ticks below represent the calculated positions of the Bragg peaks of quartz, feldspar and mica phases. Corresponding diffraction peaks are marked.

Neutron tomography

Figure 7a shows an enlarged pattern of the side slice and a three-dimensional (3D) model of the ceramic fragment 1 "Zhaipak big" reconstructed from neutron tomography data. In sample 1, an uneven spatial distribution of the neutron beam attenuation coefficients inside the volume of the fragment was observed. A well-visible layer with a high neutron attenuation coefficient on the sample surface occurs on the virtual longitudinal slices (Figure 7b). Interestingly, these areas are not detected in the optical photo. We assumed that the detected unevenness in the neutron attenuation coefficient has a chemical source. The Zhaipak monument is located near the salt lake Alakol, and, most likely, which observation areas can cause the penetration of salts and corresponding reagents during prolonged interaction of the fragment with soil or air [37, 38]. Our assumption is supported by the fact that the areas with high neutron attenuation coefficients are located mainly on the surface of the ceramic sample. The sample shows a slight presence of pores 1-3 mm in size, the total volume of which does not exceed 40 mm^3,
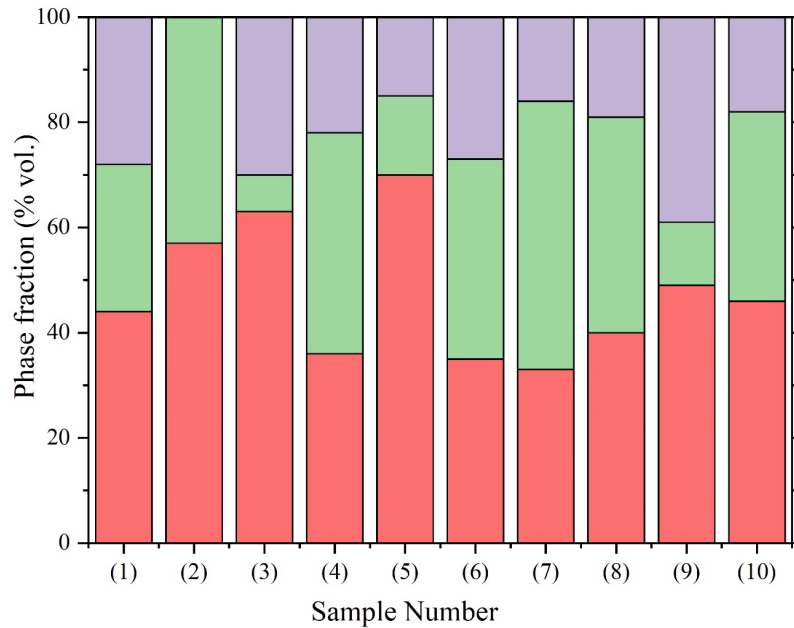
Figure 6. The bar graph shows the Rietveld fractions of quartz (red), feldspar (green) and mica (purple).

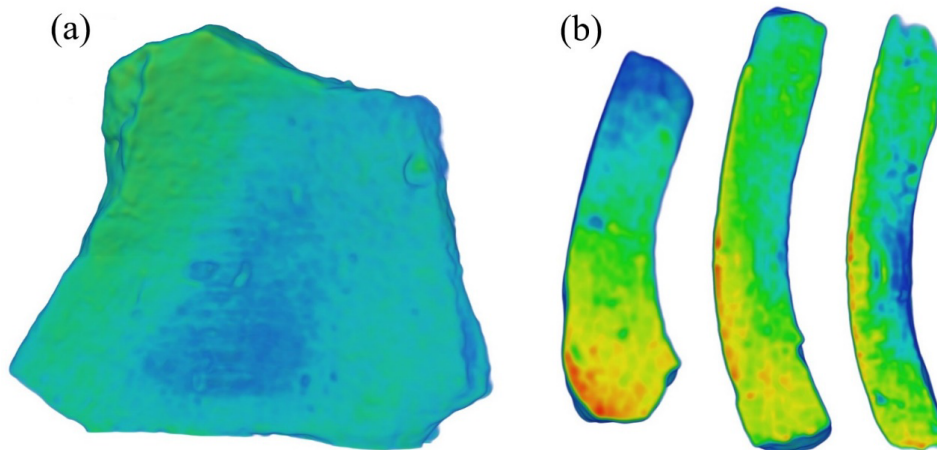which conforms to the volume of 0.98 % of the total fragment volume.

Figure 7. a) 3D model after tomographic reconstruction and b) several longitudinal slices of the 3D model of the pottery fragment. The rainbow-like coloring shows the degree of neutron absorption from low (blue color) to high (red). Regions with a high neutron attenuation coefficient can be attributed to areas with supposed salt contamination.

The optical and neutron imaging data for sample 2 "Zhaipak small" are shown in Figure 2(2) and 8. Unlike sample 1, no surface salt contamination was found in this specimen of ancient pottery. The dark color of the clay inside sample 2 indicates strong differences in the process of temperature annealing of the product. We assume that in the case of sample 2, the temperature or annealing time of the pottery product was lower than for sample 1. The reconstructed 3D model (Figure 8a) of the Zhaipak small fragment is formed by 57451192 voxels, and its volume is 8078 mm^3. The neutron tomography data of Sample 2 demonstrate the presence of several small inclusions and a branched pore structure. The pores occupy no more than 3% of the total volume of the total volume of the fragment. We assumed that the regions with high neutron attenuation coefficients

are associated with the presence of hydrogen-containing organic substances in the ceramic samples, most likely, plant sprouts or pet droppings. At the same time, the presence of plant remains was directly detected in sample Sabirbai 2(3) (see below). It is also necessary to take into account that in all the studied ceramic samples, areas of carbon were detected (see Section Raman spectroscopy), which could have been formed only as a result of combustion of organic matter during the annealing procedure.
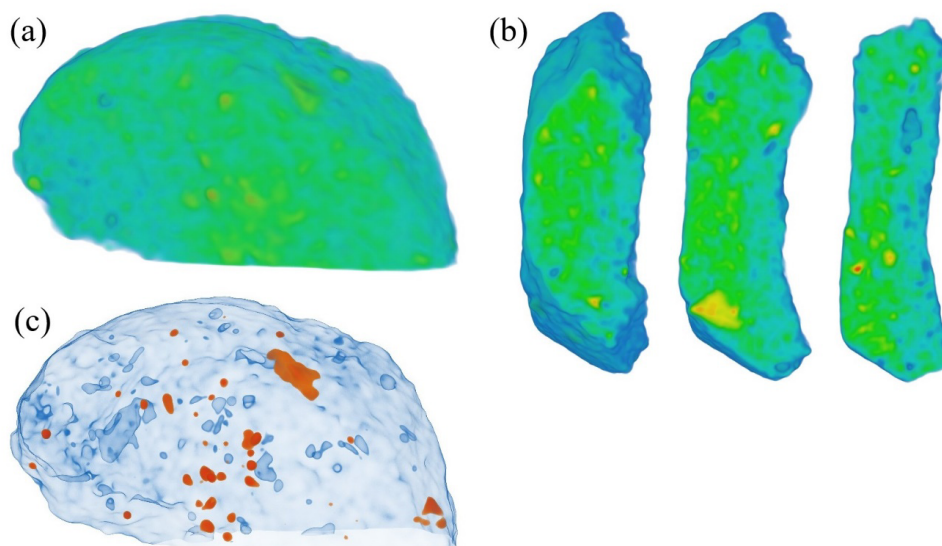

Figure 8. a) 3D model after tomographic reconstruction and c) semi-transparent representation of the 3D model with marked internal pores. b) Longitudinal slices of the 3D model of the pottery fragment "Zhaipak small". The rainbow-like coloring shows the degree of neutron absorption from low (blue color) to high (red). Regions with a high neutron attenuation coefficient can be attributed to areas with supposed salt contamination.

Two ceramics fragments of the Early Iron Age period obtained from the Tarbagatay region of the Republic of Kazakhstan were also tested using neutron methods. The obtained reconstructed 3D models of these fragments are shown in Figure 9. If a uniform distribution of components inside the volume of Eleke Sazi 6 sample, despite a slight contamination, is observed, then large areas with high neutron attenuation coefficients deep inside the volume of Eleke Sazi 5 fragment was detected. The volume of Eleke Sazi 5 sample is formed by 12359970 voxels, which corresponds to 1738 mm^3. The volume of the contaminated area is 87 mm^3. It is also necessary to note the presence of several large pores and voids with a diameter of about 0.5-3 mm, which in total occupied volume of 17 mm^3. The dark color of the slice surface of Eleke Sazi 5 sample indicates a short-term low-temperature firing in a reducing atmosphere. Whereas Eleke Sazi 6 sample belongs to fully annealed ceramics [39] and is characterized by a uniform reddish color (Figures 9b and 9d). Also, these samples are distinguished by the largest sizes of inclusions (more than 1 mm).

A ceramic fragment Ainabulak found in a Bronze Age burial mound in the Zaysan District of Kazakhstan has a relatively homogeneous base material with a small number of inclusions, but has many pores and cracks of various sizes (Figure 10). It is necessary to note the high attenuation coefficient of the neutron beam for this sample, which may indicate the presence of hydrogen-containing
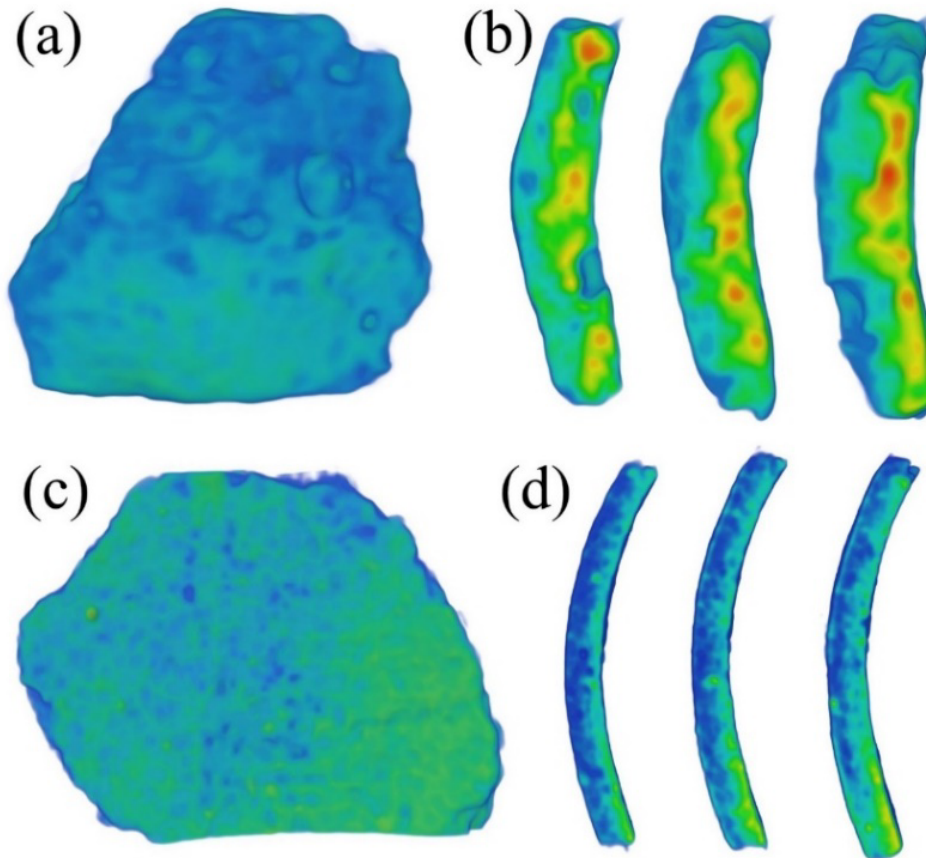
Figure 9. Reconstructed 3D models (a, c) and virtual slices (b, d) of ceramic fragments Eleke Sazi 5 and Eleke Sazi 6. The rainbow-like coloring shows the degree of neutron absorption from low (blue) to high (red).

groups and, accordingly, a low firing temperature [40]. The total sample volume is formed by 15 480 014 voxels or 2 177 mm^3. In turn, the volume of pores and cracks is about 5%.
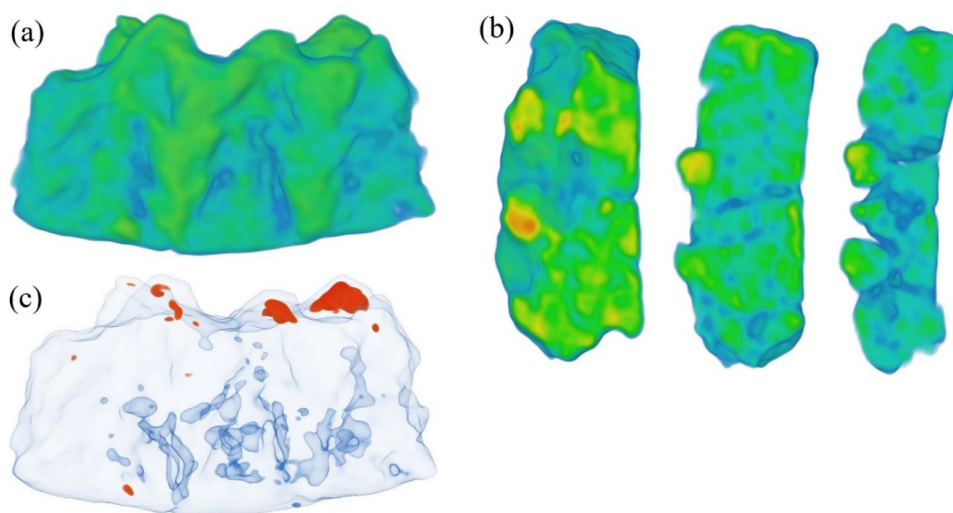

Figure 10. Reconstructed 3D model (a), several virtual slices (b), distribution of inclusions and pores (c) of the ceramic fragment Ainabulak. The rainbow-like coloring shows the degree of neutron absorption from low (blue) to high (red).

A group of Bronze Age ceramic fragments from the Tarbagatay District of Kazakhstan is characterized by the presence of a layered structure (Figure 11,

Figure 12). In the case of a two-layer structure (samples Sabirbai 2(1), Sabirbai 2(3), Sabirbai 3(C)), the outer layer has a reduced neutron beam attenuation coefficient. Slices of Sabirbai 2(2) and Sabirbai 3(A) demonstrate the presence of a three-layer structure. Two layers on the surface with a higher neutron beam attenuation coefficient and an inner layer between them with a lower one. However, it can be said that no impurities were added to the clay to impart strength, and the firing temperature was low.

The Sabirbai 3(A) and Sabirbai 3(C) samples are similar to Eleke Sazi 5 sample. There are homogeneous structures of dark color. The average attenuation coefficient of the neutron beam is higher for Eleke Sazi 5 than for Eleke Sazi 6 due to different firing temperatures. The volume of the Eleke Sazi 6 sample is formed by 30 887 588 voxels or 4 343 mm^3. The volume of the layer with an increased attenuation coefficient is 1 011 mm^3.
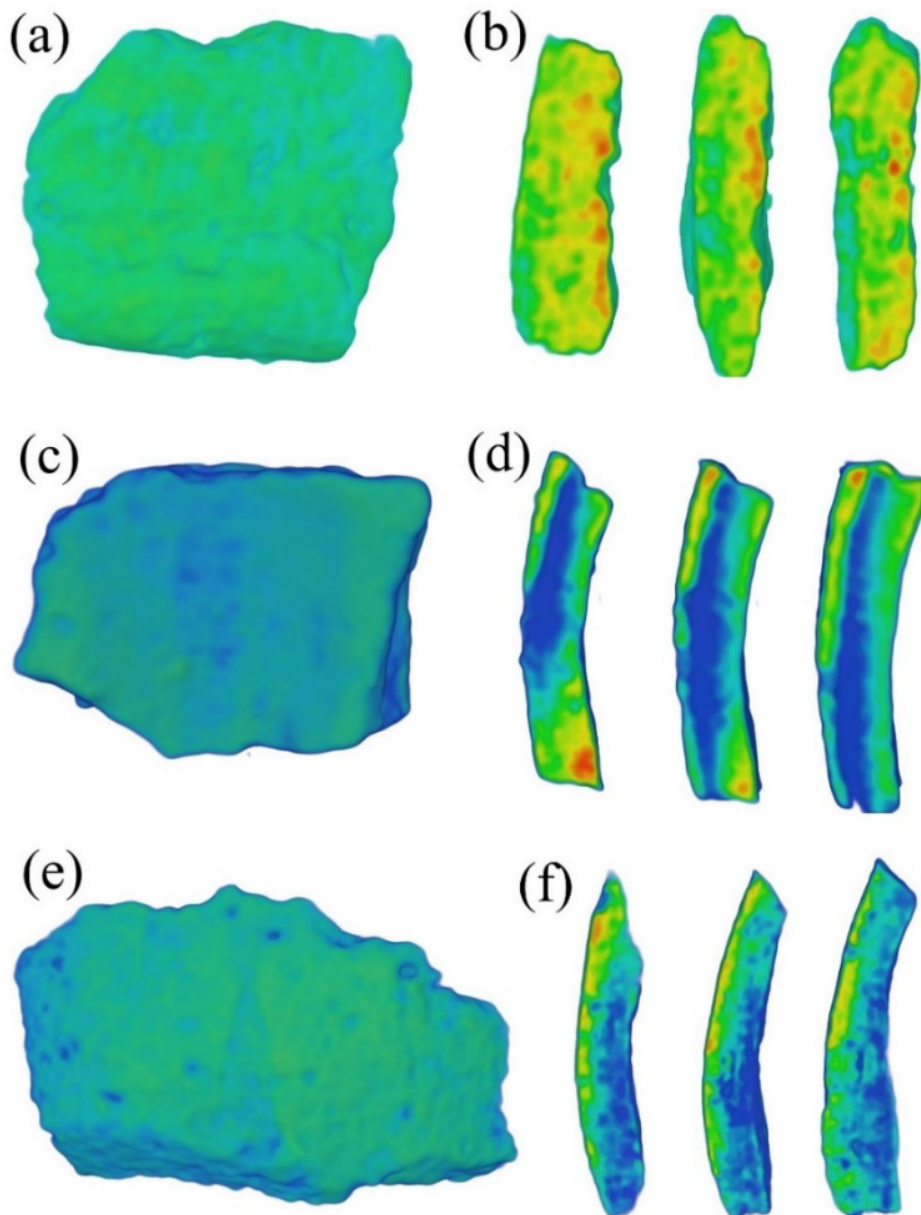

Figure 11. Reconstructed 3D models (a, c, e) and virtual slices (b, d, f) of ceramic fragments Sabirbai 2(1), Sabirbai 2(2) and Sabirbai 2(3). The rainbow-like coloring shows the degree of neutron absorption from low (blue) to high (red).
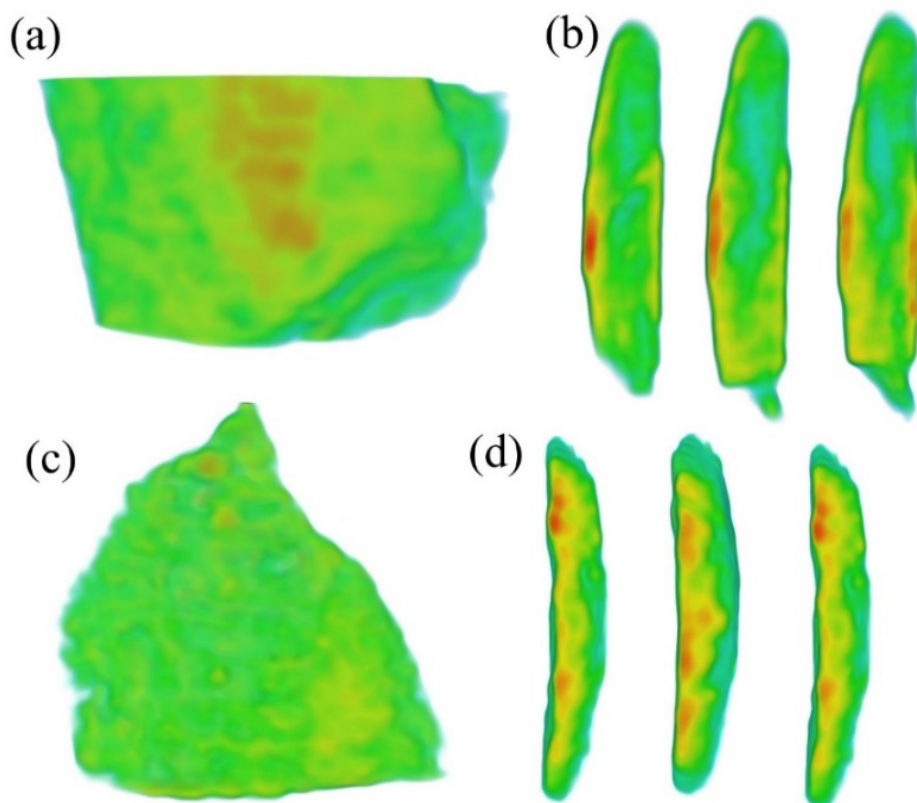
Figure 12. Reconstructed 3D models (a, c) and virtual slices (b, d) of ceramic fragments Sabirbai 3(A) and Sabirbai 3(C). The rainbow-like coloring shows the degree of neutron absorption from low (blue) to high (red).

Conclusions

The successful application of neutron methods provides new information about ancient artifacts. The unique properties of neutrons open up opportunities such as the study of ancient cities and their civilizations, which cannot be obtained by other methods. The experimental data obtained allow us to make an assumption about the recipes of molded masses for ancient pottery crafts of different eras of ancient Kazakhstan, to reveal the level of development of this craft in a specific chronological period. This means that the mineral phase composition of different ceramic materials tends to be different, which supports the concept of a fingerprint.

References

[1] P. Sciau, P. Goudeau, The European Physical Journal B **88** (2015) 132. [*CrossRef*]
[2] N. Kardjilov, G. Festa, Neutron Methods for Archaeology and Cultural Heritage (Springer, Cham, Switzerland, 2017) 349 p. [*WebLink*]
[3] D.P.S. Peacock, World Archaeology **1**(3) (1970) 375-389. [*CrossRef*]
[4] C. Andreani et al., Neutron Imaging and Applications: A Reference for the Imaging Community (Boston, MA: Springer, 2009) 229-252. [*CrossRef*]

[5] G. Festa et al., Sensors **20**(2) (2020) 502. [*CrossRef*]

[6] E.H. Lehmann et al., Nuovo Cimento Della Societa Italiana Di Fisica C **30** (2007) 93-104. [*CrossRef*]

[7] R.M. Ion et al., Applied Sciences **10**(11) (2020) 3781. [*CrossRef*]

[8] N. Kardjilov et al., Journal of Neutron Research **14** (2006) 29-36. [*CrossRef*]

[9] J. Banhart, Advanced Tomographic Methods in Materials Research and Engineering (Oxford, New York: Oxford University Press, 2008) 462 p. [*CrossRef*]

[10] W. Kockelmann et al., Journal of Archaeological Science **28**(2) (2001) 213-222. [*CrossRef*]

[11] M. Luminita, S. Florica, Journal of Engineering Studies and Research **17**(4) (2011) 73-78.

[12] B.A. Abdurakhimov et al., Journal of Archaeological Science: Reports **35** (2021) 102755. [*CrossRef*]

[13] I.P. Panyushkina et al., Radiocarbon **58** (2016) 157-167. [*CrossRef*]

[14] S. Grigoriev, Open Archaeology **7** (2021) 3-36. [*CrossRef*]

[15] A.T. Toleubaev et al., WORLD OF THE GREAT ALTAI International Research Journal **3**(4) (2017) 611-625. (ISSN 2410-2725)

[16] S.S. Chernikov, Vostochnyi Kazakhstan v epokhu bronzy [East Kazakhstan in the Bronze Age] (Moscow-Leningrad: SSSR Academy of Sciences, 1960) 272 p. [*WebLink*] (In Russian)

[17] A.T. Toleubayev et al., International Journal of Humanities and Social Sciences **7** (2013) 1874-1878. [*CrossRef*]

[18] A. Toleubayev et al., Rupkatha Journal on Interdisciplinary Studies in Humanities **12** (2020) 1-20. [*CrossRef*]

[19] A.T. Toleubayev et al., Margulanovskie Chteniya-2020: Materialy Mezhdunarodnoj Nauchno-Prakticheskoj Konferencii Velikaya Step' v Svete Arheologicheskih i Mezhdisciplinarnyh Issledovanij (Almaty, 2020) 532 p. (In Russian)

[20] D. Kozlenko et al., Crystals **8** (2018) 331. [*CrossRef*]

[21] D.P. Kozlenko et al., Crystallography Reports **66** (2021) 303-313. [*CrossRef*]

[22] J. Rodriguez-Carvajal, Physica B: Condensed Matter **192** (1993) 55-69. [*CrossRef*]

[23] B. Lafuente et al., 1. Highlights in Mineralogical Crystallography (DE GRUYTER, 2015) 1-30. [*CrossRef*]

[24] D.P. Kozlenko, Physics of Particles and Nuclei Letters **13** (2016) 346-351. [*CrossRef*]

[25] C.A. Schneider et al., Nature Methods **9** (2012) 671-675. [*CrossRef*]

[26] F. Brun et al., Advanced Structural and Chemical Imaging **3** (2017) 4. [*CrossRef*]

[27] E. Lehmann et al., Physics Procedia **88** (2017) 5-12. [*CrossRef*]

[28] E. Starnini et al., Atti Del IV Congreso Nazionale Aiar. Pisa (2007) 401-411.

[29] C. Germinario et al., Measurement **114** (2018) 515-525. [*CrossRef*]

[30] A.A. Bobrinskiy, Aktualnye problemy izucheniya drevnego goncharstva: kollektivnaia monografia (Samara: Samarskiy gos. pedagog. universitet, 1999) 233 p. (In Russian)

[31] J. Riederer, Hyperfine Interactions **154** (2004) 143-158. [*CrossRef*]

[32] P.S. Quinn, P.M. Day, Journal of Micropalaeontology **26** (2007) 159-168. [*CrossRef*]

[33] D. Deldicque et al., Carbon **102** (2016) 319-329. [*CrossRef*]

[34] L. Ghergari, C. Stancel, Studia Universitatis Babes-Bolyai, Geologia **57** (2012) 13-21. [*CrossRef*]

[35] C. Ionescu et al., Studia Universitatis Babes-Bolyai, Geologia **52** (2007) 29-35. [*CrossRef*]

[36] N. Stepanova, Teoriya i Praktika Arkheologicheskikh Issledovaniy **32** (2020) 147-156. [*CrossRef*] (In Russian)

[37] H. Morillas et al., Spectrochimica Acta Part B: Atomic Spectroscopy **146** (2018) 28-35. [*CrossRef*]

[38] C. Haldane, Topoi **6** (1996) 853-868. [*CrossRef*]

[39] S. Somiya et al., Handbook of Advanced Ceramics (Oxford: Elsevier, 2003) 187-264. [*CrossRef*]

[40] K.S. Park et al., Heritage **2** (2019) 2327-2342. [*CrossRef*]